Temporal Light Modulation: A Phantom Array Visibility Measure

J Tan, NJ Miller, MP Royer, L Irvin
Pacific Northwest National Laboratory, Portland, OR, USA

Address for correspondence: Jianchuan Tan, PhD, Pacific Northwest National Laboratory, 620 SW 5th Avenue, Suite 810, Portland OR, USA. Email: Jianchuan.Tan@PNNL.gov

This is an archival copy of an article published in *Lighting Research & Technology.* Please cite as:

Tan J, Miller N, Royer M, Irvin L. Temporal light modulation: A phantom array visibility measure. Lighting Research & Technology. Online First, April 15, 2024. doi:10.1177/14771535241239611

Abstract

At temporal light modulation (TLM) frequencies between 80 Hz and 20,000 Hz observers may perceive a series of repeated images called the phantom array effect (PAE) when they move their eyes in large saccades across a modulating light source or across a scene lit by the modulating light source. To date, there is no well-established measure for quantifying PAE visibility, but there is growing awareness of the need for one among design professionals and sensitive populations. This article documents a new measure, the phantom array visibility measure (PAVM), which is based on the results of recent human factors experiments. The measure follows the mathematical underpinning used by the flicker visibility measure (FVM) and the stroboscopic visibility measure (SVM), where the time-domain TLM waveform is converted into its Fourier frequency components; each component is evaluated through a threshold curve of modulation depth, then summed through an equation employing a Minkowski exponent. This scales the PAVM so that a value of 1 indicates a waveform at a threshold visibility in the conditions of the underlying experiment.

1. Introduction

Temporal light modulation (TLM), colloquially known as flicker, is a common but unwelcome phenomenon in LED architectural, theatrical, and automotive lighting, as well as scanners, display screens, and marker/indicator lighting.[1] Depending on the TLM frequency and waveform characteristics resulting from the dimming system and LED driver, it can manifest three different visual effects on observers.[2] At frequencies below 80 Hz, observers with a steady gaze may perceive the modulation of light as *direct flicker*, which can be quantified with measures such as short-term flicker indicator (P_{st}^{LM}),[3] perceptual modulation (M_P),[4] and flicker visibility measure (FVM).[5] At modulation frequencies between roughly 80 Hz and 2,000 Hz, the observer may see objects lit by the modulating light as having jerky or distorted movement called the *stroboscopic effect* (SE). The stroboscopic visibility measure (SVM) was developed to quantify this.[6–8] At TLM frequencies between 80 Hz and 20,000 Hz,[9] observers may perceive a series of repeated images called the *phantom array effect* (PAE) when they move their eyes in large saccades across the modulating light source or across a scene lit by the modulating light source.[10] Researchers have suggested the PAE may be associated with headaches, impaired ocular motor control, impaired visual performance, and discomfort.[1,11] However, short of a provisional model of PAE threshold visibility,[12] no measure has been proposed for quantifying the visibility of the PAE. This article documents the development of such a measure, called the phantom array visibility measure (PAVM), which is based on the data from Miller *et al.,*[13] but also informed by other recent results, such as those from Kang *et al.*[9]

The PAE is different from the stroboscopic effect in that the visibility of PAE peaks at a higher frequency than the SE and it continues to be visible by some observers well above 1,000 Hz, at which point SE is minimally visible.[1,9,11,13] Although it was hoped that SVM would work to predict PAE even though it was not designed for that purpose, Miller *et al.*[13] showed very poor correlation. Thus, a different measure is needed.

When Hershberger and Jordan[10] conducted an early study, they found that almost all participants could see the PAE in a darkened room, scanning across a light source modulating at 200 Hz, 20% duty cycle, and 100% depth. Roberts and Wilkins[1] used pulse-width modulation (PWM) control of slit-aperture sources of 120 Hz to 2,500 Hz in a dark room, with all observers able to discriminate the modulating light from steady light at frequencies averaging 1,980 Hz. Further work by Brown *et al.*[11] with a similar lighted slit against a black background in a dark room increased the average maximum frequency for visibility up to 5,800 Hz, but this extended as high as 11,000 Hz in one individual. Kang *et al.*[9] found that the PAE average visibility threshold was about 10,000 Hz for all participants, about 15,000 Hz for four highly-sensitive participants, and 19,810 Hz for the most sensitive person. These findings indicate that the PAE is visible at much higher frequencies than those explored for the SE and could explain why existing measures such as SVM are inappropriate for predicting it.

Kong *et al.* 2023[14] examined threshold visibility of a narrow source (0.2° visual angle) in dark conditions, from 80 Hz up to 1,800 Hz. They found threshold visibility of sine wave TLM was greatest around 600 Hz, where visibility occurred at modulation depths of less than 5%. Even at 1,800 Hz, threshold visibility was maintained with only 35% modulation. This suggests that the phantom array effect visibility can occur at frequencies at and above 600 Hz even when modulation depths are moderate.

The perception of the PAE is exacerbated by rectangular waveforms (*i.e.* waveforms that alternate at a steady frequency between a high and low value) with higher modulation depth.[13] These waveforms produce a temporal pattern of light not experienced in the natural world.[15] Rectangular waveforms also exhibit high-frequency Fourier content, especially those with 100% modulation and duty cycles lower than 50% because the time extent of no output over a cycle is greater when the light is only on for a short portion of each cycle, and off for the rest of the cycle. Because PWM is a common way to dim LEDs, the resulting high-frequency content enhances the PAE in TLM waveforms compared to sinusoidal TLM waveforms,[8] even when frequencies are at and possibly above 10,000 Hz.[11]

The research community is also recognizing wide variations in SE and PAE visibility among individual observers of TLM waveforms, including waveforms producing the PAE.[9,13,16] For a given waveform, the observer responses in recent studies could range from little to no detection of the effect to remarkable visual sensitivity. There are also anecdotal reports of more severe neurological responses, even if the phantom array is not consciously visible to the observer.[11]

2. Method

2.1 Data used in building PAVM

PAVM is based on data from Miller *et al*.[13] In that study, 36 participants rated the visibility of the PAE on an integer scale of 0 to 6 (where 0 = not visible at all, and 6 = very highly visible). This was done for 74 lighting stimuli with TLM characteristics varying in frequency, modulation depth, waveshape and, in the case of rectangular waveforms, duty cycle. Because an integer scale was used, and 0 corresponded to "not visible at all," the researchers held that a rating of 1 would indicate the stimulus was just visible.

There were nine sinusoidal waveforms at 100% modulation depth, with frequencies between 90 Hz and 6,000 Hz; one sinusoidal waveform at 120 Hz and 20% modulation depth; 61 rectangular waveforms with frequencies between 90 Hz and 6,000 Hz, with different modulation depths and duty cycles; and three direct current (DC) waveforms. A discrepancy existed between the Miller *et al.*[13] programmed TLM characteristics of waveshape, modulation depth, and duty cycle and the actual output from the combination of arbitrary waveform generator, laboratory driver, and LED source; so the input characteristics were modified to achieve the intended output waveforms as closely as possible. Hence, there was a slight difference between the input waveform characteristics and the output characteristics. In this article the measured output characteristics from real waveform data (not from simulations)are used in calculations. The source luminance was 38,700 cd/m^2 subtending a visual angle of 0.06° when viewed from 3 m. Total illuminance at the eye was 1.6 lx, including 1.0 lx from the source itself. The background luminance ranged from 0.6 cd/m^2 to 2.3 cd/m^2 and the task included a 44° saccade.

To assist in developing proposed specification criteria (but not in directly developing PAVM), the data from Miller *et al.*[13] was divided into two groups: all participants and higher sensitivity participants. The higher sensitivity group consists of the 18 (of 36) participants who had an individual mean rating for all 74 waveforms above the overall mean visibility rating for all observers.

2.2 Theory of PAVM

PAVM utilizes a Fourier analysis of the TLM waveform. This approach has been used in other branches of psychophysics to simulate the human nervous system's signal processing. Several researchers[8,10,17] have found this technique applicable to characterizing responses to TLM, including Wang *et al.,*[18] who showed that, like the SE, the visibility of the phantom array was higher with square waveforms than sinusoidal waveforms, so a Fourier analysis is appropriate for characterizing the response.

The approach for deriving PAVM was similar to that of SVM.[8] The basic form of the equation is expressed in Equation (1):

$$\mathit{Visibility\ Measure} = \sqrt[n]{\sum_{m=1}^{\infty}(C_m * S_m)^n} \begin{cases} < 1, & \mathit{not\ visible} \\ = 1, & \mathit{just\ visible} \\ > 1, & \mathit{visible} \end{cases} \tag{1}$$

where C_m is the amplitude of the *m^th^* Fourier component of a TLM waveform divided by the direct current (DC) value of the waveform, and S_m is the sensitivity value of visibility for a sinusoidal wave at the frequency of the m^{th} Fourier component, calculated from a frequency-domain threshold visibility function. In developing SVM, threshold visibility was defined as the percent modulation in sine wave TLM at which an individual reported seeing the SE 50% of the time. Because the data underlying PAVM did not include repeated observations to identify threshold visibility, a different determination of threshold visibility was needed: given the relatively large group of 36 study participants, 50% probability of detection within the group was regarded to be analogous to the probability gained from observations using repeated measures. That is, stimuli with 50% of participants rating the visibility as 1 or greater across the group were deemed *just visible*. Note that these waveforms also tend to have a mean visibility rating near 1.

Sensitivity values were derived by inverting the threshold values of visibility for sinusoidal waveforms. The Minkowski exponent is *n*. The steps for developing this phantom array visibility measure are illustrated in Figure 1.

Determine the threshold visibility response values for all subjects at each frequency and modulation depth. Build the visibility function from subject visibility ratings at different frequencies of square waves. The threshold modulation for each frequency occurs where 50% of subjects report visibility.

Plot the threshold visibility of each rectangular waveform by % modulation and frequency for *all* subjects. Because 100% modulation, 50% duty cycle waveforms are more visible than equivalent 100% modulation sine waveforms by a factor of 4/pi, the threshold modulation depth values for sinusoidal waves are 4/pi times more than that for rectangular waveforms. (Note: the inverse of this threshold curve is the sensitivity response curve.)

Invert the threshold data for sine waveforms to obtain sensitivity data, then plot the sensitivity curve.

Apply curve-fitting techniques to the sensitivity data plot. The resulting equation defines the sensitivity value S_m at each frequency.

Analyze the TLM test waveforms for Fourier component frequencies and normalize by dividing each component's amplitude by the waveform's DC value. This yields the Fourier component value C_m at each frequency.

This provides all input data for calculating a phantom array visibility measure value except for the exponent n, which is derived using the Minkowski method of testing data that is known to produce a target rating value around 1, as well as ~50% probability of being perceived.

Identify TLM waveforms evoking a probability of being perceived in the range of 40% to 60%. Test those waveforms in the equation using a range of exponent values (from 1.5 to 3.5 in this study). Plot the average curve of the resulting phantom array visibility values with respect to exponent values. Identify the exponent value at which the average phantom array visibility measure = 1.

Use the identified Minkowski exponent n value in the visibility measure equation along with C_m and S_m values of each TLM waveform. Compare calculated PAVM results to experimental visibility ratings (normalized by the maximum scale value, e.g. "6" in this study) to determine its predictive power.

Compare the Miller et al. responses of *higher sensitivity* subjects to *all* subjects to estimate PAVM values that may be more protective for sensitive populations.

Figure 1: Steps for developing a measure to assess phantom array visibility for a subject pool.

2.3 Determining threshold visibility curves for the phantom array effect

Given the methods and stimuli of Miller *et al.*[13], rectangular TLM waveforms were used to derive the threshold curve that relates frequency to visibility. Using spline interpolation across ratings for square (i.e., 50% duty cycle) waveforms having the same frequency, the modulation depth at which 50% of the participants would rate them visible (values ≥ 1) or not visible (values of 0) was determined. For best validity, this was done for frequencies that were presented at more than two modulation depths: 90 Hz, 120 Hz, 250 Hz, 500 Hz, 750 Hz, 1,000 Hz, and 2,000 Hz. Square waves are known to be more visible than sine waves by a factor of 4/π,[8,17,18] so threshold sine wave modulation depths were estimated by multiplying the threshold square waveform modulation depths by the amplitude ratio of $AR_{square,sine} = 4/\pi = 1.273$. The resulting thresholds of modulation depth and corresponding sensitivity values used in PAVM are listed in Table 1. The threshold data were inverted to yield sensitivity data, as shown in Figure 2, then used to derive Equation (2), which is a log-normal function. With all other factors being equal, the peak sensitivity of the PAE is predicted by PAVM to occur at 695 Hz. It is unknown how much, if at all, the frequency of peak sensitivity changes with variation in viewing or lighting conditions, such as saccade size or size of the visual target.

$$Sensitivity\ (f) = \frac{5679}{f} e^{-\frac{(\ln f - 7.987)^2}{2.885}} \qquad (2)$$

where f is the frequency.

Table 1: Thresholds of modulation depth for square and sine waves, and sensitivity values at different frequencies, for all subjects. Arbitrary units is abbreviated a.u.

Frequency (Hz)	Mod threshold for square waves (%)	Mod threshold for sine waves (%)	Sensitivity (a.u.)*
90	66.9	85.2	1.174
120	61.9	78.8	1.269
250	30.9	39.3	2.542
500	19.0	24.2	4.134
750	21.3	27.1	3.687
1,000	20.0	25.5	3.927
2,000	29.5	37.6	2.662
4,000†	48.4	61.6	1.623
6,000†	100.0	127.3	0.785

* The sensitivity data here are the inverse of modulation threshold for sine waves in percentage. The data is in arbitrary units and is not normalized. Unnormalized data provide better curve fitting.
† At 4,000 Hz and 6,000 Hz, the tested modulation depth data were not sufficient to yield a reliable estimate of thresholds. Therefore, they were excluded from the data set for sensitivity curve fitting.

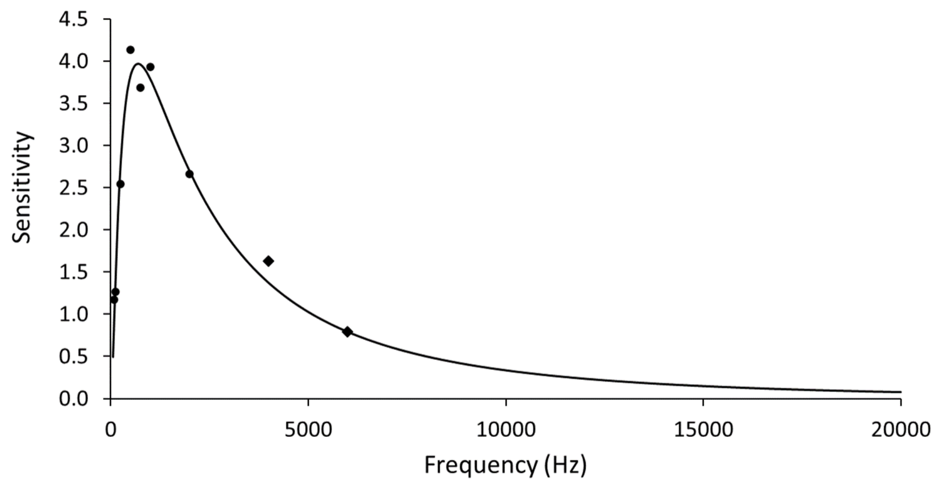

Figure 2: PAE sensitivity curve based on square TLM waveform modulation depth and frequency for phantom array effect using dataset from Miller et al.13 Notice that the y-axis is in arbitrary units (a.u.). Thus, the value 1.0 does not represent a threshold value. The two diamonds for 4,000 Hz and 6,000 Hz were added for reference, although they were not used for this curve fitting because only two modulation depth values were available, so a nonlinear interpolation was not possible—nonetheless, the curve also fits these data well.

2.4 Deriving the Minkowski exponent for PAVM

In developing PAVM, the intent was to have a PAVM value of 1 indicate visibility of a waveform for half of observers (values <1 indicate visibility for fewer than 50% of observers, and values >1 indicate visibility for more than 50% of observers). Again, this interpretation is similar to but not identical to other methods for assessing responses to TLM, such as SVM and FVM,[5-8] for which a value of 1 indicates a combination of frequency and sinusoidal wave modulation depth at which an average observer detects the TLM effect with the probability of 0.5, referred to as the detection threshold.

To achieve the intended interpretation, it was necessary to identify rectangular waveforms (but not necessarily square waveforms) that were at the threshold of visibility to half of participants, which could then be used to scale PAVM using the Minkowski exponent. Such waveforms were those with 40% to 60% of the participants providing a rating score of zero, matching the concept of “just visible” when defining PAVM. Five rectangular waveforms meeting this criterion were selected; their features are listed in Table 2.

Figure 3 illustrates the values of PAVM for the five waveforms meeting the selection criterion, calculated using a range of Minkowski exponents. The solid line shows the arithmetic mean of PAVM for all five curves. Using a second order exponential regression an n value of 2.1 was determined to produce a value of 1.

Given n = 2.1, PAVM can be explicitly expressed as shown in Equation (3):

$$PAVM = \sqrt[2.1]{\sum_{m=1}^{\infty}(C_m \cdot S_m)^{2.1}} \begin{cases} < 1, & not\ visible \\ = 1, & just\ visible \\ > 1, & visible \end{cases} \tag{3}$$

where C_m is the amplitude of the m^{th} Fourier component of a TLM waveform divided by the direct current (DC) value of the waveform, and S_m is the sensitivity value of visibility for a sinusoidal wave at the frequency of the m^{th} Fourier component, calculated from a time-domain threshold visibility function.

Table 2: Selected rectangular waveforms meeting the criterion for representing the threshold condition. These waveforms are different from those used to derive the modulation threshold curve.

Waveform	**#3**	**#19**	**#28**	**#47**	**#61**
Frequency (Hz)	90	2,000	120	120	6,000
Modulation (%)	50	50	50	50	100
Duty cycle (%)	10	10	30	50	50
Mean rating, all subjects	1.056	0.667	1.028	0.972	1.111
Probability of being visible, all subjects	50%	47%	44%	42%	50%

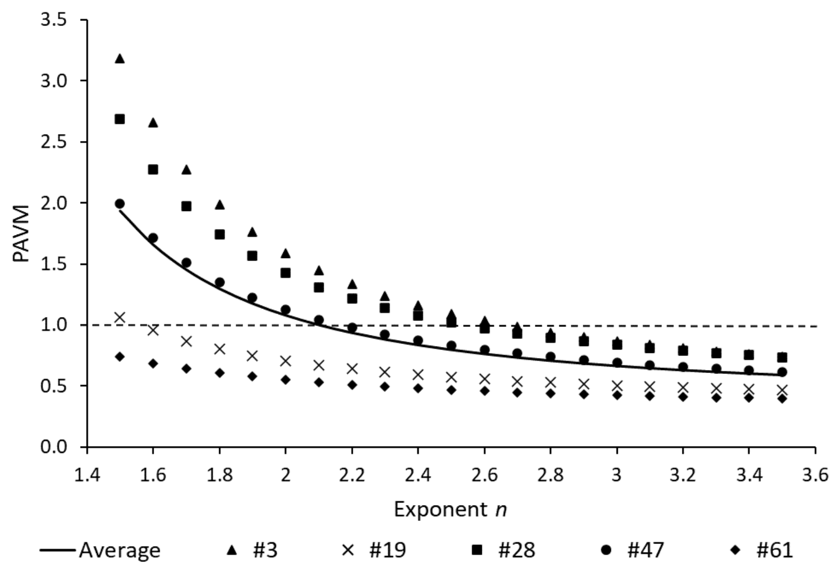

Figure 3. PAVM values vs. Minkowski exponent (n) for the selected waveforms. The "#" numbers indicate the TLM waveforms used in plotting this figure.

3. Results

Table 3 lists characteristics and PAVM values for all 74 stimuli from Miller *et al.*[13], along with their mean visibility ratings (0 to 6) normalized to a scale of 0 to 1, as well as their probabilities of being observed, for both *all* participants and the *higher sensitivity* participants. The identification of lower and higher sensitivity subjects is addressed in Section 3.1.

Figure 4 plots these data with a sigmoid trendline ($R^2 = 0.91$) for all participants. As PAVM increases, the visibility rating increases, saturating at the maximum of the rating scale. This saturation begins around a PAVM of 4, which is a region of very high PAE visibility of the TLM waveforms. Thus, an important point of interpretation is that differences in values above 4 are not of practical importance; TLM waveforms with this level of PAVM are unlikely to be acceptable in lighting applications.

Table 3. Listing of all nominal waveforms used in Miller et al.13 Note that PAVM values were calculated using real (i.e. measured output) waveform data. Also note that waveforms 53 and 55 were inadvertently programmed identically, so the visibility rating data was averaged for the two.

ID	Shape	Duty Cycle (%)	Freq (Hz)	Mod (%)	PAVM	All participants normalized mean visibility rating	High sensitivity participants normalized mean visibility rating	Probability of being observed by all participants	Probability of being observed by higher sensitivity participants
1	Rectangular	10	90	9	0.17	0.09	0.17	25%	39%
2	Rectangular	10	90	20	0.42	0.03	0.06	14%	22%
3	Rectangular	10	90	50	1.45	0.18	0.28	50%	67%
4	Rectangular	10	90	100	9.44	0.70	0.83	89%	94%
5	Rectangular	10	120	9	0.19	0.08	0.13	28%	44%
6	Rectangular	10	120	20	0.46	0.12	0.13	33%	44%
7	Rectangular	10	120	50	1.59	0.22	0.34	64%	89%
8	Rectangular	10	120	100	10.44	0.77	0.85	94%	100%
9	Rectangular	10	250	20	0.49	0.09	0.17	28%	44%
10	Rectangular	10	250	50	1.75	0.29	0.36	69%	72%
11	Rectangular	10	250	100	11.59	0.87	0.96	100%	100%
12	Rectangular	10	500	20	0.48	0.09	0.08	25%	28%
13	Rectangular	10	500	50	1.66	0.31	0.41	75%	100%
14	Rectangular	10	500	100	10.79	0.91	0.91	100%	100%
15	Rectangular	10	750	50	1.35	0.28	0.41	67%	89%
16	Rectangular	10	750	100	9.48	0.90	0.90	100%	100%
17	Rectangular	10	1,000	50	1.14	0.25	0.31	67%	78%
18	Rectangular	10	1,000	100	8.29	0.91	0.91	97%	94%
19	Rectangular	10	2,000	50	0.67	0.11	0.17	47%	61%
20	Rectangular	10	2,000	100	5.12	0.77	0.81	94%	94%
21	Rectangular	10	4,000	50	0.37	0.07	0.09	33%	39%
22	Rectangular	10	4,000	100	2.37	0.50	0.66	83%	94%
23	Rectangular	10	6,000	100	1.29	0.29	0.42	64%	78%
24	Rectangular	30	90	20	0.39	0.07	0.13	28%	39%
25	Rectangular	30	90	50	1.11	0.11	0.19	36%	44%
26	Rectangular	30	90	100	3.15	0.63	0.63	92%	94%
27	Rectangular	30	120	20	0.46	0.08	0.16	25%	44%
28	Rectangular	30	120	50	1.31	0.17	0.21	44%	61%
29	Rectangular	30	120	100	3.74	0.65	0.69	89%	94%
30	Rectangular	30	250	20	0.66	0.10	0.08	33%	39%
31	Rectangular	30	250	50	1.90	0.25	0.33	64%	78%
32	Rectangular	30	250	100	5.45	0.80	0.85	100%	100%
33	Rectangular	30	500	50	2.26	0.38	0.48	81%	100%
34	Rectangular	30	500	100	6.42	0.87	0.93	100%	100%
35	Rectangular	30	750	50	2.19	0.40	0.53	92%	100%
36	Rectangular	30	750	100	6.22	0.85	0.90	100%	100%
37	Rectangular	30	1,000	50	2.00	0.42	0.57	83%	94%
38	Rectangular	30	1,000	100	5.68	0.81	0.84	100%	100%
39	Rectangular	30	2,000	50	1.24	0.30	0.48	67%	89%
40	Rectangular	30	2,000	100	3.53	0.73	0.82	100%	100%
41	Rectangular	30	4,000	100	1.53	0.45	0.59	86%	94%
42	Rectangular	30	6,000	100	0.75	0.26	0.38	69%	94%
43	Rectangular	50	90	20	0.35	0.10	0.19	22%	44%
44	Rectangular	50	90	50	0.88	0.12	0.20	36%	39%

45	Rectangular	50	90	100	1.86	0.56	0.61	83%	89%
46	Rectangular	50	120	20	0.42	0.08	0.15	28%	50%
47	Rectangular	50	120	50	1.05	0.16	0.25	42%	50%
48	Rectangular	50	120	100	2.22	0.64	0.72	89%	89%
49	Rectangular	50	250	20	0.64	0.16	0.26	36%	56%
50	Rectangular	50	250	50	1.60	0.34	0.42	83%	94%
51	Rectangular	50	500	100	4.27	0.81	0.87	100%	100%
52	Rectangular	50	500	50	2.01	0.37	0.52	83%	100%
53	Rectangular	50	750	100	4.28	0.77	0.87	94%	100%
54	Rectangular	50	750	50	2.02	0.37	0.54	78%	100%
55	Rectangular	50	750	100	4.28	0.77	0.87	97%	100%
56	Rectangular	50	1,000	50	1.88	0.40	0.57	81%	94%
57	Rectangular	50	1,000	100	3.99	0.79	0.90	97%	100%
58	Rectangular	50	2,000	50	1.21	0.32	0.45	72%	78%
59	Rectangular	50	2,000	100	2.54	0.67	0.85	94%	100%
60	Rectangular	50	4,000	100	1.07	0.37	0.51	78%	89%
61	Rectangular	50	6,000	100	0.53	0.19	0.27	50%	72%
62	DC	100	90	0	0.00	0.10	0.18	31%	39%
63	DC	100	120	0	0.00	0.05	0.07	19%	28%
64	DC	100	1000	0	0.00	0.06	0.08	22%	33%
65	Sine	N/A	90	100	0.81	0.26	0.32	19%	28%
66	Sine	N/A	120	20	0.19	0.06	0.10	67%	83%
67	Sine	N/A	120	100	1.46	0.34	0.39	78%	94%
68	Sine	N/A	250	100	2.93	0.57	0.69	92%	100%
69	Sine	N/A	500	100	4.02	0.68	0.81	92%	100%
70	Sine	N/A	750	100	4.10	0.70	0.80	94%	100%
71	Sine	N/A	1,000	100	3.85	0.67	0.75	100%	100%
72	Sine	N/A	2,000	100	2.45	0.55	0.69	89%	100%
73	Sine	N/A	4,000	100	0.99	0.31	0.43	67%	89%
74	Sine	N/A	6,000	100	0.50	0.09	0.11	39%	56%

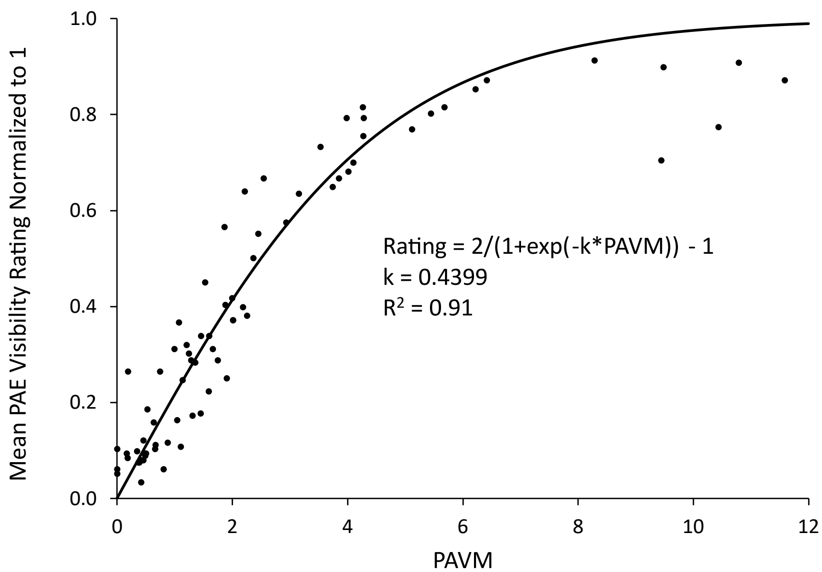

Figure 4. The correlation between normalized rating scores of all 74 waveforms from all subjects and their PAVM values calculated from real waveform data.

3.1 Interpretation of PAVM values and establishing specification criteria

Proper interpretation of PAVM values is critical to its implementation. As with SVM, P_{st}^{LM}, M_P, and FVM, PAVM values are tied to the experimental conditions that underlie the measures, including source size, luminance contrast of the target against its background, relative movement, and saccade speed. Thus, measures that address visibility of TLM-induced effects cannot predict visibility at an absolute level for actual lighting installations, nor for an individual observer. Nonetheless, they are useful for comparing relative performance of different products. Using a value of one to anchor the measures is a consistent and logical choice, but it does not need to also be the recommended limit for specifications. A value lower than one can further reduce phantom array visibility for more people and/or address more problematic viewing conditions.

We believe setting target values to address visibility for more sensitive population groups is critical and is in alignment with recently adopted European regulations.[19] This recognizes that more sensitive populations need additional protection so that they are not excluded from common daily environments and activities. Although there are extreme neurological conditions that are difficult to understand medically, groups such as migraineurs are more sensitive to more extreme modulating light sources—migraineurs make up 6% to 9% of men and 18% to 26% of women in the US and Canada, totaling almost 50 million adults in 2011.[20] Because these individuals participate fully in public lighted environments, the PAVM and its recommended values are intended to predict visibility from a more sensitive subject pool.

Although PAVM and its underlying threshold/sensitivity functions are based on a broad sample of people, an appropriate criterion less than 1 can be used to address more sensitive people, because the sensitivity functions for higher-sensitivity people do not substantially differ in shape from that for all people. That is, the peak sensitivity is largely unchanged, with only the magnitude of sensitivity changing.

In the Miller *et al*. study,[13] 36 participants completed the Leiden Visual Sensitivity Scale questionnaire[21] and were evenly divided into either the higher or lower sensitivity group according to their summed responses. Unfortunately, many of the subjects reported high sensitivity through the Leiden scale questions, but that was inconsistent with their responses. In developing recommended PAVM criteria, a simple arithmetic mean of individual participant responses to all 74 TLM waveforms was used to identify participants as higher or lower sensitivity.

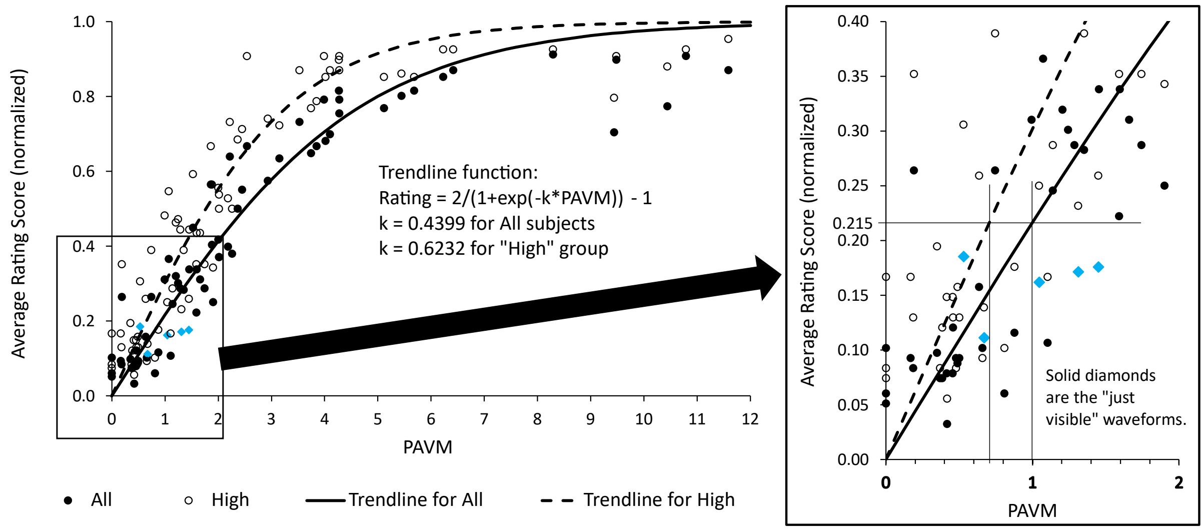

Figure 5: Normalized visibility ratings of all and higher sensitivity subjects against calculated PAVM values derived from all subjects (left) and magnification of plot near origin (right). The solid diamonds indicate the five "just visible" waveforms listed in Table 2.

Figure 5 shows the normalized visibility ratings of all and higher sensitivity participants of Miller *et al.*, plotted against PAVM values. The solid black trendline in Figure 5 is fit to the arithmetic mean ratings from all subjects. The dashed black trendline is fit to the arithmetic mean rating for the 18 higher sensitivity subjects. At PAVM = 1.0, the corresponding visibility rating calculated from the sigmoid function fit to the *all* data is 0.215. At the same visibility rating for the *higher* sensitivity data, the corresponding PAVM is approximately 0.7. Therefore, a PAVM value of 0.7 indicates approximately half of the higher sensitivity people (or around 25% of all people) would find the PAE to be visible in viewing conditions like the underlying experiment—this is not particularly protective. Further, it is important to note that migraineurs were excluded as subjects in the Miller et al. study—a limitation similar for the studies that underlie M_P, SVM, and FVM.[22,23] Given this limitation, the *all* group is not truly representative of all people, and a stimulus with a value of 1 may be visible to more than half of people. Given these factors, a maximum PAVM value of *less* than 0.7 should be considered for use in lighting specifications when PAE is a concern for occupants. Just as regulatory groups are using lower values of SVM (0.4) to protect highly sensitive populations, a PAVM value such as 0.5 might protect most people in most cases, but the exact value is subject to further refinement.

By design, SVM and PAVM values have compatible interpretations, allowing them to be used together to specify limits on the stroboscopic effect and phantom array effect.

3.2 Stability of PAVM as a measure

In past work,[24] the stability of multiple flicker measures was investigated at different sampling rates. It is essential for a measure to be stable (*i.e.,* have consistent values) with varying sampling rates arising from different measurement devices. If a measure is not stable across sampling rates, the calculated values might vary from lab to lab or from instrument to instrument, for the same TLM waveform.

To explore its sampling rate stability, PAVM was calculated for 208 digitally simulated (*i.e.,* not measured from real) waveforms, at a combination of 13 frequencies, 4 modulation depths, and 4 duty cycles—the same set used in Tan *et al*.[24] For each waveform, a series of 7 sampling rates (in the unit of kilo samples per second (abbreviated here as kS/second for brevity)) was used, as shown in Table 4. The target for percent variation in PAVM across sampling rates was <10% for any PAVM values > 0.1, with difference determined by the minimum and maximum values at the given sampling rate and higher (*i.e.* $[PAVM_{max} - PAVM_{min}] / PAVM_{max} < 10\%$). That is, the variation for 100 kS/second was determined from difference of the extremes of calculated PAVM values using 100 kS/second, 200 kS/second, and 400 kS/second.

When using a sampling rate at 200 kS/second or higher, all PAVM value variations were below 10% for PAVM values > 0.1. When sampling rate was higher than 100 kS/second, PAVM values for almost all waveforms varied by less than 10%; a typical exception occurred on the simulated waveform with fundamental frequency of 8,000 Hz, modulation depth of 100% and duty cycle of 10%. This waveform's variation in PAVM was 24.2% when sampled at 100 kS/second but dropped to 1.74% when sampled at 200 kS/second and above. The absolute values of the calculated PAVM were at 1.28 for sampling rate of 100 kS/second, 0.97 for 200 kS/second, and 0.97 for 400 kS/second. Another typical exception happened on the simulated waveform with fundamental frequency of 10,000 Hz, modulation depth of 100% and duty cycle of 10%. This waveform's variation in PAVM was 30.3% when sampling rate at 100 kS/second but dropped to 9.78% when sampled at 200 kS/second and above. The PAVM values were 0.98 for sampling rate of 100 kS/second, 0.75 for 200 kS/second, and 0.68 for 400 kS/s. The two exceptions have PAVM values around the threshold level for both the *all* and *high-sensitivity* populations. An ideal sampling rate is high enough that the PAVM value will not vary across the threshold value. Based on these data and the extreme examples, a minimum sampling rate of 200 kS/second is recommended for the PAVM. This sampling rate is higher than what is recommended for many other flicker measures,[4,25,26] but is to be expected given that the PAE can be visible at much higher frequencies.

Table 4: The parameters of digitally simulated (i.e., not real) waveforms and the sampling rates used to evaluate these waveforms for stability of calculated PAVM.

Parameters	Values
Frequencies (Hz)	80, 100, 120, 200, 400, 600, 800, 1,000, 2,000, 4,000, 6,000, 8,000, 10,000
Modulation depths	10%, 20%, 60%, 100%
Duty cycles	10%, 30%, 50%, 90%
Sampling rates (kS/second)	10, 20, 40, 80, 100, 200, 400

4. Discussion

4.1 Comparisons

PAVM is the first proposed measure for characterizing the PAE, so it is not possible to make direct comparisons to other measures. However, the CIE 249:2022[12] describes a provisional temporal contrast threshold (*i.e.* temporal modulation depth threshold) for the PAE (Equation 4). According to Perz *et al.*,[8] sensitivity corresponds to the inverse of a modulation depth threshold visibility curve; therefore, a sensitivity curve can be derived by $S = 1/T$.

$$T_v = 75.06e^{-0.004f} + 6.86e^{0.001f} \tag{4}$$

where T_v is the threshold visibility, f is the frequency of waveform. The sensitivity is the inverse of that equation.

In the visibility measure equation from CIE 249:2022, the Minkowski exponent was set at $n = 4$. To compare the functions of Equation (4) and Equation (3), the sensitivity curve provided in CIE 249:2022 was normalized and compared with a normalized sensitivity curve generated from Equation (3), as shown in Figure 6. Any overall sensitivity differences due to different experimental viewing conditions is not captured in this figure due to the normalization; such differences must be disregarded for product-level metrics anyway.

The sensitivity curve produced by Equation (3) peaks at 695 Hz, while the CIE sensitivity curve peaks at around 750 Hz; this may be due to different viewing conditions and experimental protocols that underlie the two functions, or simply variation in the underlying sample of observers. Recent work from Kong et al. found peak sensitivity even lower, around 600 Hz.[14] The more important difference occurs at frequencies away from the peak, particularly above about 4,000 Hz, where the sensitivity function underlying PAVM shows much higher sensitivity and is in better agreement with recent data.[9,11,13] Notably, sensitivity functions based on waveform characteristics alone must be created from a dataset of consistent lighting and viewing conditions, because factors such as source size or luminance contrast affect relative visibility. It is not currently possible to combine datasets to cover a wider frequency range without sufficient data to account for the effects of viewing and lighting conditions of PAE visibility.

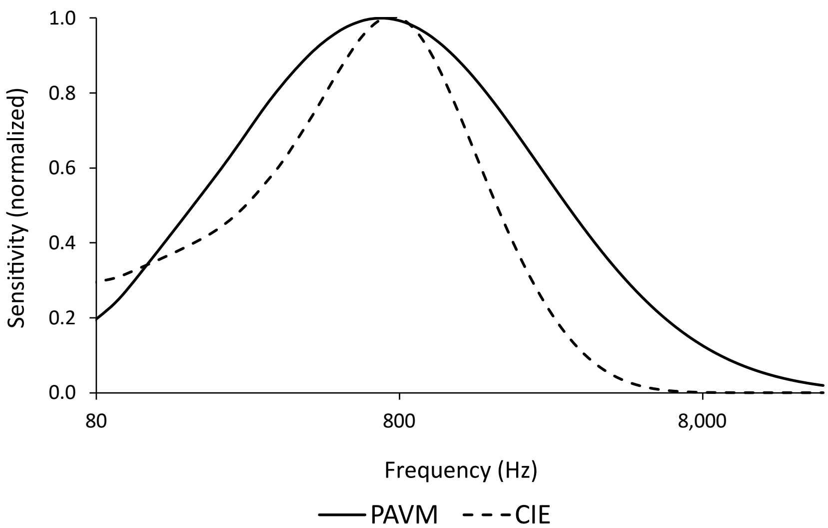

Figure 6: The normalized phantom array effect sensitivity curves derived from Miller et al.13 (solid) and CIE 249:202212 (dashed).

The threshold modulation depths (i.e., the modulation depth at a given frequency that is just visible) of sinusoidal waveforms from both PAVM and CIE can also be compared, as shown in Figure 7, (only the threshold values up to 100% are plotted). The CIE curve, based on the work of Wang et al. 2019[27] used a narrow white target (0.02° visual angle) on a black background on a table lighted to 250 lx or 500 lx. The TLM conditions were 100 Hz, 600 Hz, 1200 Hz; sine waves; modulation depths of 20%, 30%, 50%, 70%, and 100% for 100 Hz and 1200 Hz; modulation depths of 8%, 10%, 12%, 15%, and 20% for 600 Hz; the averaged visibility thresholds were deduced from the modulation depth corresponding to 75% of the correct detection rate. This data produced a minimum threshold of 18.3% modulation, while the PAVM curve has minimum threshold of 25.2% modulation. The difference is not unexpected, given the different lighting and viewing conditions in the two underlying studies.

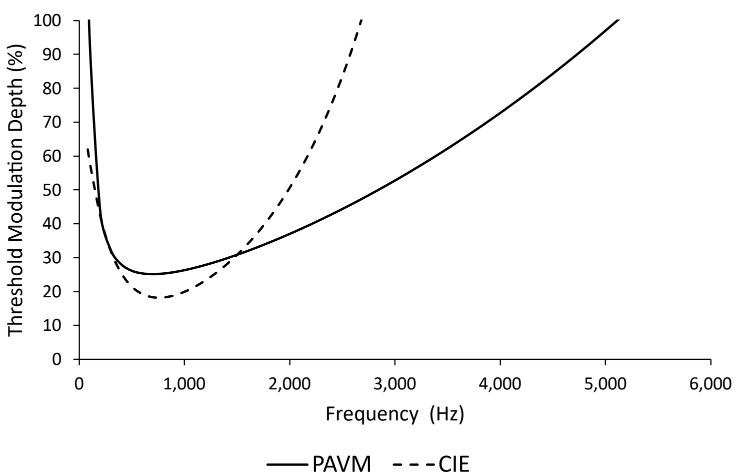

Figure 7: The threshold modulation depth curves derived for PAVM and CIE 249:202212 (dashed).

PAVM can be used to address TLM at much higher frequencies than are of concern for direct flicker and the SE. It can effectively complement the stroboscopic visibility measure (SVM), which if used alone may increase the prevalence of light sources producing a PAE, since it was never designed to predict phantom array visibility, or address TLM at frequencies above 2,000 Hz.[13]

Eliminating all responses to TLM simultaneously can be achieved by avoiding all frequencies below approximately 25,000 Hz. This assumption is based on the elimination of visible light responses to TLM in the 1990s in the US when there was a rapid transition to high-frequency electronic ballasts operating at 30–60 kHz.[28] However, cost, efficiency, size, and other factors may preclude this approach to designing drivers and dimmers. This is where PAVM, in combination with other measures addressing the SE and direct flicker, can be useful in ameliorating undesirable effects from TLM.

4.2 Limitations

Overall, the performance of PAVM—and the underlying findings of Miller *et al.*[13]—build on and improve understanding of the phantom array effect visibility as reflected in the body of literature.[1,9,11,16,18,29,30] The modulation depth threshold visibility function, and its inverse sensitivity function, are informed expansions of the provisional model introduced in CIE 249:2022,[12] which was based on a more limited and unpublished data set.

One limitation of the approach used to develop the PAE modulation depth threshold visibility function is that it was not identical to that used in similar studies for the SE and direct flicker effect. Instead of repeated conditions to determine threshold visibility for individual subjects, a threshold function was determined using the interpolated point estimating 50% probability of visibility across the sample population. A conversion factor was used to convert square wave visibility to equivalent sine wave visibility. Furthermore, threshold visibility was determined by the researchers as a value of 1 on a 0 to 6 integer rating scale where 0 was no visibility and 6 was high visibility. Not all participants necessarily assigned a value of 1 to a point of just barely visible. Additional research will help define the sensitivity curve with greater precision and align the PAVM sensitivity curve with those developed for the SVM and M_P.

This article describes an early PAVM model. More work from other laboratories is needed to confirm its performance and/or identify potential improvements. Additional research on visibility of the PAE under different viewing conditions; a wider array of waveform characteristics; larger and more varied population samples; and stimuli of varying size, luminances, and contrasts with background will help test the performance and widen the applicability of PAVM. PAVM will be improved by conducting experiments with *a priori* hypotheses generated using PAVM values and associated criteria.

5. Conclusion

This article proposes a new measure for assessing the visibility of the phantom array effect (PAE) in response to temporal light modulation (TLM). A sensitivity function for phantom array visibility was developed using recently published data from Miller *et al.*[13] for 90 Hz up to 2,000 Hz. This function was evaluated further by ensuring its high-level agreement with additional PAE visibility data from Miller et al. and Kang et al.[9] that found the mean visibility for higher sensitivity subjects to be 15,100 Hz.

PAVM was developed emulating similar psychophysical approaches used to develop other TLM measures, utilizing the Minkowski norm. PAVM was based on mean visibility ratings from 36 experiment participants and is scaled so that a value of 1 predicts about half of people will see the PAE in conditions matching the underlying experimental data. Values lower than 1 indicate visibility for fewer people, and higher values indicate visibility for more people.

Visibility of the phantom array effect varies substantially from person to person; more sensitive individuals are more likely to see the phantom array effect at any given PAVM value, and some neurologically highly sensitive individuals may need even more restrictive environmental lighting conditions. In the interest of protecting more sensitive subjects from annoyance, distraction, cognitive effects, nausea, migraines, and other potential health effects resulting from exposure to TLM, visibility ratings from the 18 higher sensitivity participants were compared to those of all participants. At a PAVM value of 0.7, the arithmetic mean visibility ratings for the higher sensitivity group corresponded to average ratings of 1.0 for all participants. Consequently, a maximum PAVM of 0.7 is provisionally recommended for architectural and vehicular lighting applications—but is still expected to result in PAE visibility for about 25% of people. Recalling that migraineurs were excluded as subjects from the Miller et al. study, these data may not reflect the responses of the highest sensitivity groups. A lower maximum PAVM, such as 0.5, would be expected to minimize PAE visibility for most people in a wider range of applications. Further validation is warranted to determine whether this value is too conservative or not conservative enough to prevent unwanted responses from TLM.

The stability of PAVM at different sampling frequencies and its sensitivity to deviations in waveforms was also investigated. For PAVM values greater than 0.1 (i.e., the region of practical interest for relative stability), PAVM was found to be stable within a range of +/- 10% when using a sampling rate of 200 kS/second, which is thus the minimum recommended value.

In the future, it will be important to examine the performance of PAVM using datasets other than the one that underlies its development—and for which it *should* perform well. This is challenging to do at present because waveform data from past experiments are not publicly available.

Funding

This work was supported by the U.S. Department of Energy's Lighting R&D Program, part of the Building Technologies Office within the Office of Energy Efficiency and Renewable Energy (EERE).

Acknowledgment

Eduardo Rodriguez-Feo Bermudez at PNNL provided the real output waveform data used in the study. Felipe Leon at PNNL provided great review comments to this paper.

References

1. Roberts JE, Wilkins AJ. Flicker can be perceived during saccades at frequencies in excess of 1 kHz. *Lighting Research and Technology* 2013; 45: 124–132.

2. Commission Internationale de l'Eclairage. *Visual aspects of time-modulated lighting systems – Definitions and measurement models*. TN006:2016. Vienna, Austria, 2016.

3. International Electrotechnical Commission. *Equipment for general lighting purposes – EMC immunity requirements – Part 1: Objective light flickermeter and voltage fluctuation immunity test method.* IEC TR 61547-1. Geneva, Switzerland, 2020.

4. ASSIST Recommends. *Recommended metric for assessing the direct perception of light source flicker*. Lighting Research Center, Rensselaer; 2015; 3(1).

5. Perz M, Sekulovski D, Vogels I, Heynderickx I. Quantifying the Visibility of Periodic Flicker. *Leukos* 2017; 13: 127–142.

6. Vogels I, Sekulovski D, Perz M. Visible artefacts of LEDs. In: *Proceedings of 27th Session of the CIE*. Sun City, South Africa, 2011: 42–51.

7. Sekulovski D, Perz M, Vogels I. Modeling the visibility of the stroboscopic effect. In: *Proceedings of the CIE Symposium on Lighting Quality and Energy Efficiency*. Hangzhou, China, 2012: 439–449.

8. Perz M, Vogels IMLC, Sekulovski D, Wang L, Tu Y, Heynderickx IEJ. Modeling the visibility of the stroboscopic effect occurring in temporally modulated light systems. *Lighting Research and Technology* 2015; 47: 281–300.

9. Kang HR, Lee CS, Lee JM, Lee KM. Phantom array effect can be observed above 15 kHz in high speed eye movement group for high luminance warm white LED. *Lighting Research and Technology* 2023. First published Jan 20. DOI:14771535221147312.

10. Hershberger WA, Jordan JS. The phantom array: A perisaccadic illusion of visual direction. *Psychol Rec* 1998; 48: 21–32.

11. Brown E, Foulsham T, Lee CS, Wilkins A. Research Note: Visibility of temporal light artefact from flicker at 11 kHz. *Lighting Research and Technology* 2020; 52: 371–376.

12. Commission Internationale de l'Eclairage. *Visual Aspects of Time-Modulated Lighting Systems*. CIE 249:2022. Vienna: CIE. 2022.

13. Miller NJ, Rodriguez-Feo Bermudez E, Irvin L, Tan J. Phantom array and stroboscopic effect visibility under combinations of TLM parameters. *Lighting Research and Technology.* Online first, 2023; DOI:14771535231169904.

14. Kong X, Vogels R, Martinsons C, Tengelin MN, Heynderickx I. *Dependence of Temporal Frequency and Chromaticity on the Visibility of the Phantom Array Effect. Proceedings of the Commission Internationale de l'Eclairage (CIE) Conference 2023*, Ljubljana Slovenia. Vienna: CIE, 2023, 347-356.

15. Wilkins A. Fear of light: On the cause and remediation of photophobia. *Lighting Research and Technology* 2021; 53: 395–404.

16. Park SW, Lee CS, Kang HR, Pak HS, Wilkins A. Visibility of the phantom array effect according to luminance, chromaticity and geometry. *Lighting Research and Technology* 2020; 52: 377–388.

17. Campbell FW, Robson JG. Application of fourier analysis to the visibility of gratings. *Journal of Physiology* 1968; 197: 551–566.

18. Wang LL, Yu X, Tu Y, Perz M, Sekulovski D. *Influence of Frequency, Waveform and Colour on the Visibility of the Phantom Array Effect. Proceedings of the Commission Internationale de l'Eclairage (CIE) Conference 2018,* Taipei, Vienna, CIE, 2018, 138–146.

19. European Union (EU) Commission. Commission Regulation (EU) 2019/ 2020 of 1 October 2019 laying down ecodesign requirements for light sources and separate control gears. Publications Office of the European Union.

20. Stokes M, Becker WJ, Lipton RB, Sullivan SD, Wilcox TK, Wells L, et al. Cost of health care among patients with chronic and episodic migraine in Canada and the USA: Results from the international burden of migraine study (IBMS). *Headache* 2011; 51: 1058–1077.

21. Perenboom MJL, Najafabadi AHZ, Zielman R, Carpay JA, Ferrari MD. Quantifying visual allodynia across migraine subtypes: The Leiden Visual Sensitivity Scale. *Pain* 2018; 159: 2375–2382.

22. Bodington D, Bierman A, Narendran N. A flicker perception metric. *Lighting Research and Technology* 2016; 48: 624–641.

23. Perz M. Modelling visibility of temporal light artefacts. PhD dissertation. Technische Universiteit Eindhoven. 2019.

24. Tan J, Leon F, Miller N. Temporal Light Modulation: Data Processing and Metric Calculations. *Lighting Research and Technology.* First published Jun 18, 2023; DOI:14771535231172085.

25. California Energy Commission. *California Title 24 Appendix JA10 test method for measuring flicker of lighting systems and reporting requirements. California: Building Energy Efficiency Standards*. Sacremento, California, 2016.

26. National Electrical Manufacturers Association. *Temporal Light Artifacts: Test Methods and Guidance for Acceptance Criteria.* NEMA 77-2017. Rosslyn, Virginia, 2017.

27. Wang LL, Tu Y, Cheng SL, Yu XL, Perz M, Sekulovski D. *The visibility of the phantom array effect under office lighting condition. Proceedings of the Commission Internationale de l'Eclairage (CIE) Conference, 2019, Washington DC*. Vienna: CIE, 2019, 17-21. DOI:10.25039/x46.2019.OP03.

28. Lehman B and Wilkins AJ. Designing to Mitigate Effects of Flicker in LED Lighting: Reducing risks to health and safety. *IEEE Power Electronics Magazine*. Sept 2014; Vol. 1, no. 3, pp. 18-26. DOI: 10.1109/MPEL.2014.2330442.

29. Kang HR, Kim JG, Park SW, Lee CS, Pak H. Visibility of the phantom array effect at different LED colour temperatures under high-frequency temporal light modulation. *Lighting Research and Technology* 2023; 55(1):36-46.